Total and elastic cross-sections for electron and positron scattering from OCS molecule: A comparative study with CO_2

O. Sueoka, A. Hamada, and M. Kimura
Graduate School of Engineering, Yamaguchi University, Ube, Yamaguchi 755, Japan

H. Tanaka and M. Kitajima
Department of Physics, Sophia University, Tokyo 102, Japan

(Received 1 February 1999; accepted 7 April 1999)

We have carried out a joint experimental and theoretical study on determination of total and elastic cross-sections for electron and positron impact on OCS molecules. For total cross-section measurements, impact energies are from 0.7 to 600 eV for electron collisions and 0.8 to 600 eV for positron collisions. For elastic scattering, only electron impact has been studied from 1.5 to 100 eV. Our present measurements for total cross-sections for electron impact are found to agree extremely well with the measurements of Dababneh *et al.* (1982) in the entire energy region studied. The results by Szmytkowski *et al.* (1994) are consistently larger by 20% above 2 eV, and, in particular, are larger by a factor of two in the 1.2 eV resonance region. The present theory for elastic scattering is in good agreement with the present measurement, and has been employed for understanding the dynamics. The total cross-section recommended here is probably the best in accuracy as of today although further studies would be helpful. © *1999 American Institute of Physics.*
[S0021-9606(99)01725-0]

I. INTRODUCTION

As a part of our ongoing investigation and evaluation of total, elastic, and inelastic cross-sections, we have earlier conducted a systematic effort for determination of accurate total and elastic cross-sections for carbon dioxide (CO_2).[1] Due to its fundamental nature as well as numerous applications from astrophysics and aeronomy to plasma chemistry, the CO_2 molecule remains important, and accurate recommended cross-section data are urgently required for applications.

As our second effort, we have selected OCS molecule. The reasons are twofold: (i) OCS is a linear molecule like the CO_2, but unlike CO_2, it has a permanent dipole moment (0.712D), and the comparison of all aspects of dynamics with CO_2 would be of interest; (ii) two sets of experimental total cross-sections by electron impact previously reported disagree with each other, and furthermore, one theoretical attempt does not offer much help in resolving the controversy. This molecule is known to be present in interstellar clouds, and hence, knowledge of the cross-section is certainly relevant to astrophysics.

There have been four experimental[2–4] investigations for total cross section of the molecule based on electron beam and one theoretical study[5] based on the continuum multiple-scattering (CMS) method. Although the theoretical study has given clear indications of the origin of shape resonances in electron scattering, unfortunately, agreement between the various experiments as well as between theory and experiment is as yet unsatisfactory for practical use especially at energies below 100 eV. Some remarks on these discrepancies are in order, and further thorough investigation from the experimental and theoretical side would be desirable.

To investigate more thoroughly the dynamics in electron scattering from OCS, it is important to examine the problem using a different probe such as positron scattering. There has been no experimental attempt reported so far for positron scattering. From the theoretical point, electron and positron interactions with a target molecule can be approximately represented by the static, exchange, and correlation–polarization terms. For electron impact, the static and correlation–polarization interactions are both attractive, and exchange interaction plays an important role when the incident electron energy is low. These three interactions contribute in a rather complex manner to scattering. For positron scattering, the static interaction is repulsive, while the correlation–polarization interaction is attractive, and no exchange interaction exists, and hence, the repulsive static and attractive polarization interactions cancel out, resulting in a smaller effect on the scattering at low-to-intermediate energies. As the incident energy increases above 100 eV, interactions become more perturbative and the Born-type perturbative approaches are known to be valid and frequently used for describing scattering dynamics. Such approaches lead to similar magnitudes of cross-sections for both projectiles.[6] Therefore, by studying these two-projectile cases closely, we could learn more details of the interactions and underlying dynamics.

In this note, we report our measurements of the total cross-sections (0.7–600 eV), elastic cross-section (1.2 eV–100 eV), and results of theoretical calculations (1.0–100 eV) for the elastic process. These results are compared with experimental and theoretical results published earlier to identify the cause of discrepancies, and to obtain a ''realistic'' estimate of the total cross-section. We also carry out a comparative study between OCS and CO_2 molecules so as to comment on the similarity and difference in the cross-

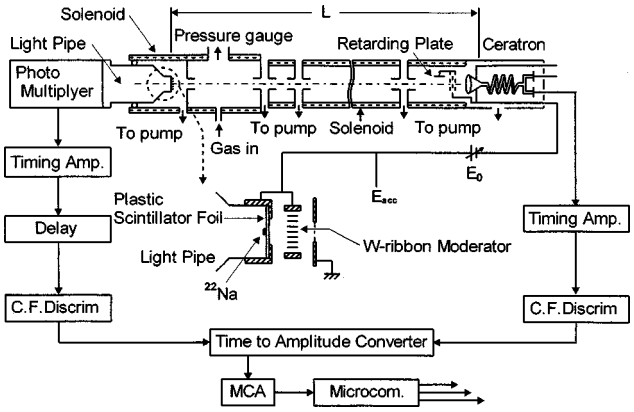

FIG. 1. Schematic diagram of the apparatus and the main electronics. A nonuniform axial magnetic field is applied by solenoid coils.

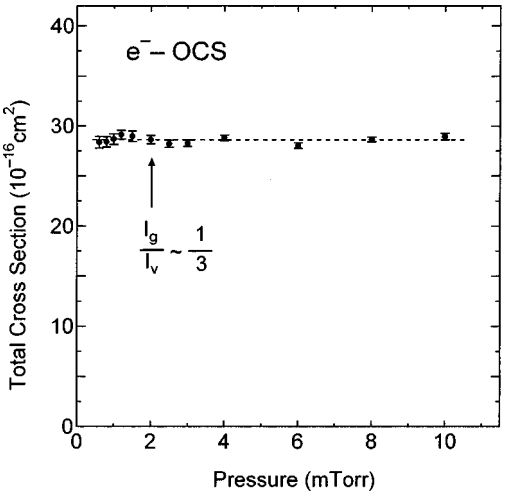

FIG. 2. Total cross-sections for electrons plotted against collision gas pressure. The beam-intensity attenuation (I_g/I_v) of 1/3 is shown by an arrow. Error bars show only the statistical error.

sections. Furthermore, it has been known for CO_2 and other molecules[6] that the total cross-section by electron impact, which is generally larger than that of positron impact, reverses with that of positron impact in the energy region near 1–2 eV. In this energy region, rovibrational excitation channels may be responsible for the reversal of these cross-sections. It would be interesting if this same effect can be observed in the OCS.

II. METHODS

A. Total cross-section (TCS) measurement

The TCS measurements for positron and electron collisions were performed using the same absorption-type apparatus and almost the same experimental procedure as previously.[7] The β^+ decay radioisotope ^{22}Na with an activity of 80 mCi and a tungsten-ribbon moderator are used as the positron source and the moderator, respectively. Slow electron beams with an energy width of around 1 eV were produced from secondary electrons emitted from the isotope via multiple-scattering in the W-moderator. The experimental set up is schematically shown in Fig. 1. The energy spectrometer employed time-of-flight (TOF) detection. A retarding potential was applied to the TOF system to eliminate elastically and inelastically scattered projectiles. All measurements were carried out automatically. The purity of the OCS gas was 97.5%, although the higher purity is more ideal. TCS values Q_t are obtained from the absorption coefficient in the following equation.

$$I_g = I_v \exp(-Q_t n l), \tag{1}$$

where n and l are the number density in the collision cell and the effective length of the cell, respectively. I_v and I_g are the incident beam intensity and that after passing through the gas run, respectively. The effective length of l was determined by the normalization to the $e^+ - N_2$ cross section data of the Wayne State Univ. group.[8] The value of Q_t as the absorption coefficient is independent on the gas pressure in principle. The gas-pressure independence of Q_t was checked as shown in Fig. 2.

In this experimental condition, the effect of the forward scattering is fairly large, because of the wide exit-aperture of the collision cell and of using the magnetic field for the transportation of projectiles. The effect for a forward peaking scattering depends strongly on the shape of differential elastic cross sections (DCSs) used, and was examined based on the simulation method.[9] Unfortunately, two sets of the data for the DCSs measured by the present investigation[10] and Sohn *et al.*[11] are quite different in angular dependence. For low-energy scattering, the present DCS data are rather flat toward low angles, while the DCSs of Sohn *et al.* show a sharp increase with decreasing angle at low energies. The maximum difference between the two is approximately a factor of two below 40° at energy less than 5 eV. Hence, it is interesting to examine the effect of the DCS used for evaluating the TCS, which were obtained by using two different sets of DCSs: (a) the present DCSs by the CMS, and (b) the present experimental DCSs.[10] The results were plotted in Fig. 3 along with those uncorrected as a reference. The varia-

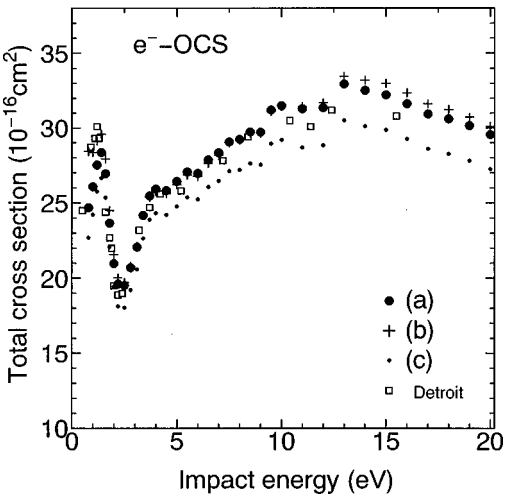

FIG. 3. Examples of the sensitivity of the total cross-sections to different DCS data. (a) The present DCSs by the CMS, (b) the present experimental DCS data [below 1.5 eV, the DCSs by Sohn *et al.* (Ref. 11) were adopted (see details in Ref. 10)], and (c) without correction.

tion in DCSs is found to affect the TCS determination but the effect is small with the deviation less than 10% in the entire energy region. As a further check, we have adopted the DCSs by Sohn *et al.*[11] Although at certain angular regions, the difference in DCSs is large, this does not directly carry through the TCS calculation, however. The TCSs evaluated by using various DCSs agree well within 15%. Hence we can safely conclude that the TCSs are not much affected by the choice of DCSs used. Note that the experimental data shown in Figs. 4–9 below have been determined by inclusion of forward scattering by the case (c).

Estimation of the error was performed by addition of $\Delta n/n$, $\Delta I/I$, $\Delta l/l$, where I is $\ln(I_v/I_g)$, and ΔI includes all statistical errors in the count including the error due to the background. The value of $\Delta l/l$ is around 2% for positron collisions, while it is about 0.5–1% for electron collisions. The error arising from the gas density, Δn, almost depends on the sensitivity of the pressure gauge (CMH4-M11 of Vacuum General); $\Delta n/n$ is 0.3% depending on the collision gas pressure. The error due to the normalization procedure for the determination of the effective length $\Delta l/l$ was estimated to be 2%. The errors in the experimental data of Hoffman *et al.*,[7] which was used in the normalization process, are not included in the present estimate of our error. The numerical data with corresponding errors described above are included in Table I.

TABLE I. Numerical data for total cross-sections of OCS by electron (Q_1^-) and positron (Q_1^+) impact. The number in the bracket, (x), represents the absolute value of the error in ($\pm x$).

E (eV)	Q_1^- (10^{-16} cm^2)	Q_1^+ (10^{-16} cm^2)
0.7	···	11.2(1.0)
0.8	24.7(1.2)	···
1.0	26.1(1.1)	14.6(0.9)
1.2	27.5(1.1)	···
1.3	···	15.7(0.9)
1.4	28.4(1.2)	···
1.6	26.9(1.1)	15.8(0.9)
1.8	23.7(1.0)	···
1.9	···	16.3(0.9)
2.0	21.0(0.9)	···
2.2	19.6(0.8)	16.1(0.9)
2.5	19.5(0.8)	15.2(0.9)
2.8	20.7(0.9)	15.2(1.0)
3.1	22.1(0.9)	15.3(1.0)
3.4	24.2(1.0)	15.5(1.0)
3.7	25.5(1.1)	16.6(1.0)
4.0	25.9(1.1)	16.9(0.9)
4.5	25.8(1.1)	17.2(0.9)
5.0	26.4(1.1)	17.9(1.0)
5.5	27.1(1.1)	17.7(1.0)
6.0	27.0(1.1)	19.3(1.1)
6.5	27.9(1.2)	18.9(1.0)
7.0	28.3(1.2)	18.7(1.1)
7.5	29.1(1.3)	19.2(1.1)
8.0	29.2(1.3)	18.9(1.1)
8.5	29.7(1.3)	19.8(1.2)
9.0	29.7(1.3)	18.9(1.2)
9.5	31.2(1.4)	19.5(1.3)
10.0	31.5(1.3)	18.8(1.2)
11.0	31.3(1.4)	20.2(1.1)
12.0	31.4(1.4)	20.1(1.2)
13.0	32.9(1.4)	20.5(1.3)
14.0	32.5(1.4)	20.0(1.4)
15.0	32.2(1.4)	20.3(1.3)
16.0	31.6(1.4)	19.7(1.4)
17.0	30.9(1.4)	20.5(1.3)
18.0	30.6(1.4)	19.6(1.4)
19.0	30.2(1.3)	20.7(1.4)
20.0	29.5(1.3)	20.2(1.6)
22.0	29.2(1.3)	19.8(1.2)
25.0	27.5(1.2)	20.0(1.3)
30.0	26.7(1.2)	19.3(1.0)
35.0	25.4(1.1)	···
40.0	24.9(1.2)	18.4(1.1)
50.0	22.8(1.1)	17.7(1.0)
60.0	21.1(1.0)	17.2(1.0)
70.0	20.0(0.9)	15.6(1.0)
80.0	19.0(0.9)	15.0(0.9)
90.0	17.9(0.8)	14.3(0.9)
100.0	16.9(0.8)	13.8(0.9)
120.0	15.6(0.7)	12.7(0.8)
150.0	14.0(0.6)	12.1(0.7)
200.0	12.4(0.5)	10.0(0.7)
250.0	10.6(0.5)	9.6(0.7)
300.0	9.8(0.4)	8.4(0.6)
400.0	8.4(0.3)	7.3(0.4)
500.0	7.4(0.3)	6.4(0.5)
600.0	6.4(0.3)	5.4(0.4)

B. Positronium (Ps) formation measurement

In the energy dependence of the total cross-section for rare gases, a sudden increase of the cross-section is clearly seen just above the Ps formation threshold.[6–8] This increase is apparently caused by Ps formation. For some polyatomic molecules studied by this group, however, this distinct feature does not necessarily appear, or the feature is significantly weakened or washed out. In order to estimate the Ps formation cross section, an alternative type of experiment was performed on the basis of the combination of the total cross-section experiment of the conventional absorption type described above and the Ps formation experiment earlier developed in this group.[7] Specifically, the absorption-type total cross section experiment was carried out with a stronger magnetic field (approximately 31 G). The contribution of the Ps formation was found enhanced in the total cross-section curve, because the forward scattering was increased further by the stronger magnetic field. Inelastic cross-sections other than the Ps formation are assumed to monotonically increase around the Ps formation threshold as a function of the incident energy. Hence, by subtracting these inelastic cross-sections from the measured total cross-section, the Ps formation cross-section can be extracted with reasonable accuracy at, at least, a few eV above the threshold of the Ps formation.[6] An example of the present Ps formation cross-section will be shown and discussed later.

C. Differential elastic cross-section (DCS) measurements

The experimental arrangement and procedures used in the present DCS measurements, as well as the determination of integrated elastic cross-sections were similar to those of previous studies.[12–14] The experimental DCSs have been measured from 20° to 130° between 1.5 and 100 eV incident electron energy. Elastic cross sections are determined by in-

tegration of the DCS over the scattering angle. The DCSs for $\theta<20°$ and $\theta>130°$ are obtained by the extrapolation based on the data of the present CMS calculation. Details of the method and procedure will be provided in the forthcoming paper that is concerned with DCSs only.

D. The continuum multiple scattering method

The theoretical approach used is the continuum multiple-scattering (CMS) method, which is a simple but efficient model for treating electron scattering from polyatomic molecules.[15,16] To overcome difficulties arising from (i) the many degrees of freedom of electronic and nuclear motions, and (ii) the nonspherical molecular field in polyatomic molecule, the CMS divides the configuration space into three regions: Region I, the atomic region surrounding each atomic sphere (spherical potentials), region II, the interstitial region (a constant potential), and region III, the outer region surrounding the molecule (a spherical potential). The scattering part of the method is based on the static-exchange-polarization potential model within the fixed-nuclei approximation. The static interaction is constructed from the electron density obtained from the CMS wavefunction, and the Hara-type free-electron gas model[15,16] is employed for the local-exchange interaction, while the dipole and polarization interactions are treated via terms proportional to r^{-2} and r^{-4}, respectively. A simple local-exchange potential replaces the cumbersome nonlocal exchange potential making the calculation tractable.

Under these assumptions, the Schrödinger equation in each region is solved numerically under separate boundary conditions. By matching the wavefunctions and their derivatives from each region, we can determine the total wavefunction of the scattered electron and hence, the scattering *S*-matrix. Once the *S*-matrix is known, then the scattering cross-section can be easily calculated. This approach has been tested extensively and is known to provide useful information on the underlying scattering physics.[15] Further, the CMS method is useful for interpolation and extrapolation for guiding experimental data points. Note that the present method and that by Dill and Dehmer is basically the same, but more elaborate potentials and wavefunctions were employed in the present study, which are mainly responsible for some differences in the cross-section seen below.

For later discussion, some of known threshold energies for vibrational excitations are provided here:[16]

vibrational excitation: $(100)=0.107\,\text{eV}$,
$(010)=0.064\,\text{eV}$,
$(001)=0.256\,\text{eV}$.

For electronic excited states, very little is known, and there is no systematic assignment of electronic states.

III. RESULTS

First, we discuss the results for electron scattering, and those for positron scattering. We divide our discussion for scattering into three specific scattering-energy regions, namely, (a) the higher energy region above $E>7$ eV where electronic excitation channels begin to open, (b) the intermediate energy region which covers a prominent resonance peak ($2\text{ eV}<E<7\text{ eV}$: dominant inelastic processes are vibrational excitation), and (c) the low energy region below 2 eV. We also make some remarks on the comparison with CO_2 at each section. Lastly, we compare the results for electron and positron scattering. In this approach, we hope that we could illustrate agreement and deviation between experiments and theories, and suggest a recommended set of the total cross-section data, which we believe to be the most accurate to date.

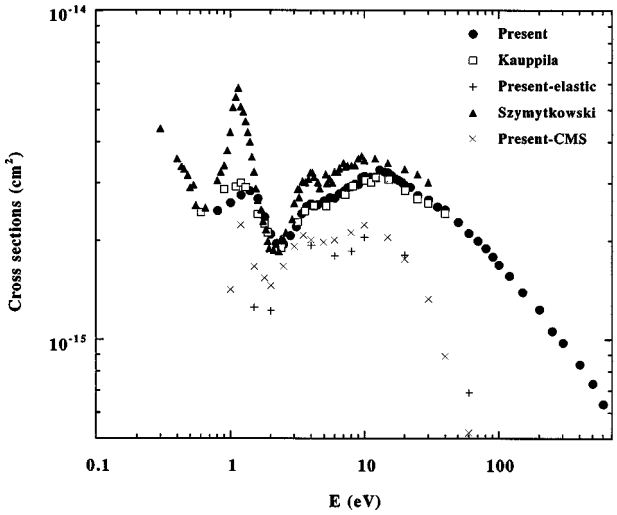

FIG. 4. Total and elastic cross-sections for electron scattering. The data shown are indicated in the figure. The present theoretical results are for *elastic scattering*, and all others are for total cross-sections.

A. Electron impact

Figure 4 shows all total and elastic cross-sections for electron impact based on experimental and theoretical studies.

1. High-energy region

TCS observed by the present study agrees nearly perfectly with the data by Dababneh *et al.*[2] in magnitude and energy dependence at all energies. The data by Dababneh *et al.* lie within the lower end of the present error bars. The TCS data by Zecca *et al.*,[3] and Szymytkowski *et al.*[4] are also found to be in reasonable accord with ours and those by Dababneh *et al.* above 10 eV to 30 eV, although they are slightly larger by 15%. The present theoretical results for elastic scattering are slightly larger than the present elastic measurement above 12 eV,[12] but are in reasonable accord in the energy dependence. The elastic cross-sections drop sharply above 10 eV because it becomes weaker at higher energies, and inelastic channels including ionization and several electronic excitations begin to dominate. It is natural to expect that electronic excitation processes begin to increases rapidly as soon as they pass threshold energies ($E_{th}>7$ eV) and reach the cross section as large as $\geqslant 10^{-16}\,\text{cm}^2$ at a few tens of eV. Good agreement of the present theoretical results for elastic scattering also supports the reasonable accuracy of our measured elastic cross-section. The strong peak at 12 eV

is due to shape resonances from various partial wave contributions from σ to δ waves, but a major player here is the d wave as pointed out earlier by Lynch *et al.*[5] based on their CMS calculation.

2. Intermediate energy region

The present total measurements are found to agree perfectly with those of Dababneh *et al.*[2] in this energy region, which are nearly identical. Both results show a shoulder at around 3.5 eV, which is characterized as the combination of σ and δ wave contributions. But this shoulder is secondary compared to the larger and broader peak at around 15 eV. In our analysis based on the CMS, the contribution from δ partial wave solely dominates, giving a smaller peak than that by Lynch *et al.* Then both drop rather rapidly toward the minimum at 2 eV. The data by Zecca *et al.*, and Szmytkowski *et al.* are found to be consistent in shape with ours and those of Dababneh *et al.* in this energy domain. However, their magnitude is again slightly larger than ours and that of Dababneh *et al.* Their resonance peak at 3.5 eV is found to be more conspicuous and stronger than the present. This difference may be due to the finer resolution used by Zecca *et al.* and Szmytkowski *et al.*, although they begin to approach ours and those of Dababneh *et al.* as the incident energy decreases below 3 eV. The present elastic data are smaller by 30%–40% from the present total cross-sections in 5–7 eV, while the difference shrinks somewhat at the peak position of the resonance at 3.5 eV. In the lower end of this energy region, vibrational excitation should be dominant, although some electronic excitation particularly for triplet-state formations, which possess lower threshold energies, may still be possible. These channels account for the difference between the total and elastic cross-sections.

3. Low energy region

The present measurement is in excellent agreement with those by Dababneh *et al.*[2] although the level of agreement somewhat decreases below 1.5 eV. Below 1.5 eV, the present results and those of Dababneh *et al.* begin to deviate slightly with the maximum difference of 15%. The peak near 1.2 eV is clearly visible in both, and the origin of the peak is due to the π wave shape resonance as identified by Lynch *et al.* earlier. This peak seen by Zecca *et al.*, and Szmytkowski *et al.* is much larger and stronger by a factor of two to three than ours although their position seems to match well with the present result. The present elastic results at 1.5 and 2 eV are found to be rather small, and may be somewhat underestimated. Although below 1–2 eV vibrational and rotational excitations are most likely to be dominant inelastic processes, it seems unlikely that these rovibrational excitations amount to approximately $1.6\times10^{-15}\,\mathrm{cm}^2$ (the difference between the total and elastic cross-sections) at 1.5 eV to fill the gap. The theoretical elastic result is slightly larger by 30% than the measurement, while that by Lynch *et al.* is much larger by a factor of two than the present. The origin of the discrepancy in two theories may be due to the different treatment of molecular states and interactions. Electron dissociative attachment (DA) channel should be present in this energy domain, but no details are yet known. More careful study on the DA would be very interesting and important for applied fields such as plasma processing since the electron energy loss process competes with the DA.

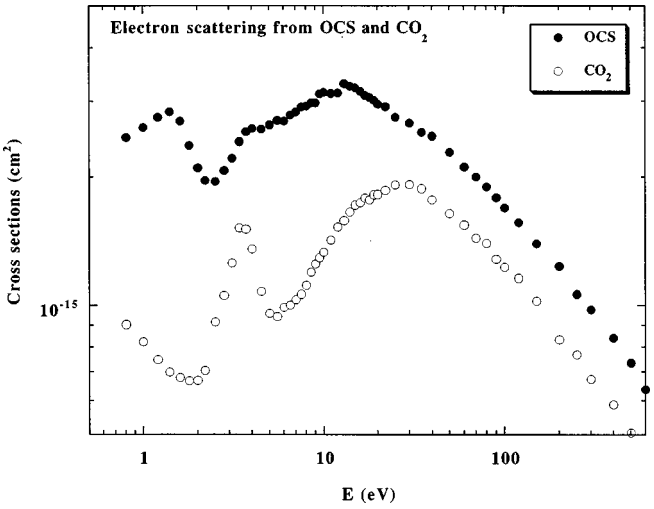

FIG. 5. A comparison between two total cross-sections for OCS and CO_2 by electron impact.

4. Comparison with CO_2

Detailed comparison between the TCSs for OCS and CO_2 is shown in Fig. 5. General features in TCSs for OCS and CO_2 are much similar. A broad maximum for the OCS and CO_2 is seen at around 15 eV, and 30 eV for OCS and CO_2, respectively, followed by monotonic decrease on the higher energy side. However, the magnitude for the OCS is larger by 24% above 100 eV. The origin of this difference reflects the size of the molecule, i.e., the bond length of the C–S bonding is approximately 2.9415 a_0, while that for the C–O bonding is 2.1962 a_0. The C–S bond length is roughly 25% longer than that of the C–O bonding. Incidentally the difference in the two cross-sections, which amounts to about 24%, corresponds nearly identically to the size of the molecule. This broad hump at 12 and 30 eV for OCS and CO_2 is due to the shape resonance through the combination of σ, π, and δ partial waves. A shoulder seen at 3.5–4.0 and 8 eV for OCS and CO_2 is due to the δ wave contribution. The sharp resonances at 1.4 and 3.6 eV for OCS and CO_2, respectively, are known to arise from shape resonances of $^2\Pi$ configuration of temporary negative ions. All peak positions for OCS shift toward the lower energy side, in comparison with those for CO_2, owing to lower energy levels in a S atom. Because of its permanent dipole moment, the total cross-section for OCS should turn around and increase as the incident energy decreases below ~1 eV. This trend is, in fact, seen in the experimental result by Szmytkowski *et al.* below 0.5 eV. In summary, the general features in the TCS are found to be very similar except for the magnitude and energy shift, reflecting the size and the electronic nature of the molecule.

B. Positron impact

Figure 6 shows TCSs from the present positron measurement. There are no other experimental results for this molecule with which to compare.

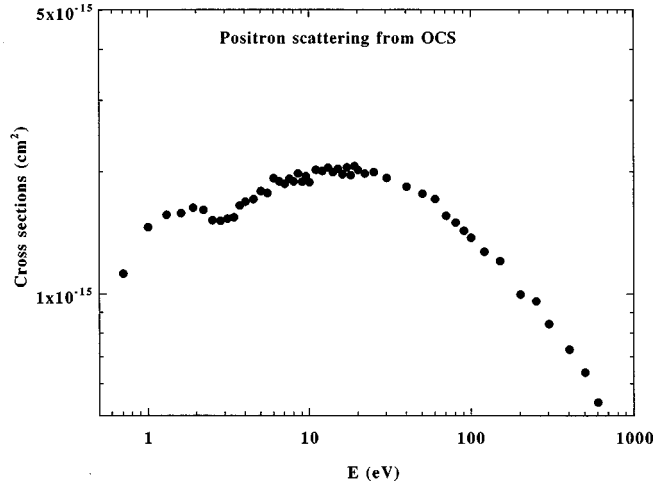

FIG. 6. Total cross-sections for OCS by positron scattering. The data shown are indicated in the figure.

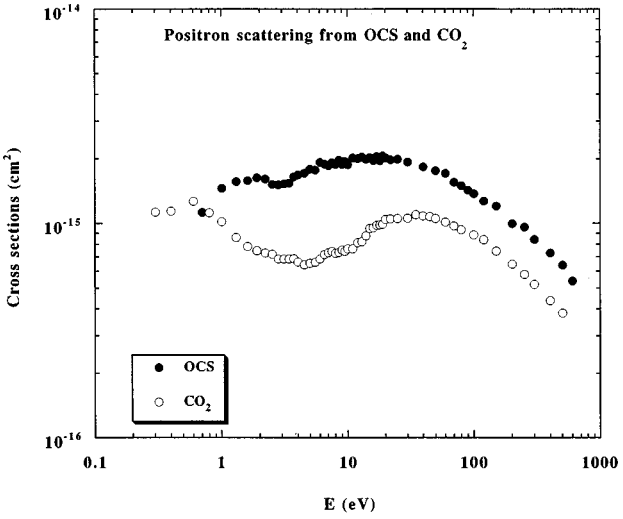

FIG. 7. A comparison of total cross-sections between OCS and CO_2 by positron impact.

1. High energy region

The present results show small oscillatory structures in the entire energy region; a small structure at 11 eV corresponds to the opening of OCS ionization channels, and that near 7.8 eV to positronium formation. Even at the highest energy of 600 eV studied, the positron scattering and electron scattering cross-sections do not exactly begin to merge. This feature is clearly different from the CO_2 case, where they are found to merge around 200 eV. We have noticed in some systems earlier that as the molecular size increases, the energy region where the two cross-sections begin to merge shifts toward higher energies.[1] This is clearly a breakdown of the simple first-order perturbation theory, and it may require higher-order corrections as the molecular size and hence, a number of electrons increases for the convergence of the cross-section calculation. A small hump around 40 eV is interesting, and we speculate that the origin of this hump may be due to a new opening of another ionization channel.

2. Intermediate energy region

The resonance peak seen in electron impact at around 3.8 eV is not present, of course, in positron impact, reflecting clearly the different interaction mechanism and energy dependence between incoming positron– and electron–nuclear motions. The positron scattering results gradually decreases from the peak at around 20 eV, and reaches a minimum around 2.5 eV. Interestingly, this minimum point coincides with that for electron scattering. From the theoretical point of view, there is no reason that both electron and positron scattering cross-sections should behave similarly at this energy region, and hence, this similarity may be accidental in a sense that three interaction terms in electron scattering and two interaction terms in positron scattering coincide in this energy region.

3. Low energy region

A broad but conspicuous peak at around 1 eV is obvious, and we tentatively conclude that positron attachment may well be its origin. We notice that as the molecular size increases, the more often the broad structure shows up near 1–2 eV region.[6] The electron cloud in a molecule ''swarms'' toward the incoming positron and wraps it up, forming a temporal bound state within the molecule. This is characteristically another type of a shape resonance. In order to examine the origin of this broad peak above, it is extremely interesting to carry out further detailed experimental study for much lower energies. Below the peak at 1 eV, the cross-section begins to decrease at much lower energies. However, because the OCS is a polar molecule, the total cross-section should back up and begin to increase, which is a characteristic feature of a polar molecule. Where they change slope is an interesting question, and further experimental and theoretical study is warranted.

4. Comparison with CO_2

Detailed comparison between the TCS for OCS and CO_2 is shown in Fig. 7. Generally the TCS of OCS is rather flat with weak structures at 1.5 and 20 eV, as discussed, while that of CO_2 has two visible strong structures at 0.6 and 30 eV. Like TCSs for electron scattering, these structures for OCS appear to shift toward the lower energy side. The minimum at around 4 eV for CO_2 is much deeper than the corresponding minimum for OCS. An interesting characteristic is the behavior below 1 eV, where the TCS for OCS appears to decrease at much lower energies, while that for CO_2 becomes the plateau, hence reversing the magnitude of the two TCSs at around 0.8 eV. Since OCS is a polar molecule, the TCS should increase as the energy is lowered. But at 0.8 eV, it has not reached that point yet.

5. Positronium (Ps) formation

Figure 8 shows the Ps formation cross-section as a function of incident energy. The arrow in the figure indicates the threshold of the Ps formation, E_{Ps}, and its value is approximately 4.4 eV. The Ps formation increases gradually as the incident energy increases, and the cross-section reaches a value of $1.8\times10^{-16}\,\mathrm{cm}^2$ at 6.4 eV. The contribution of the Ps

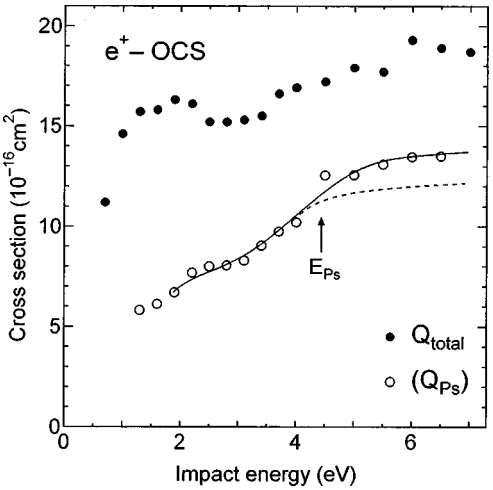

FIG. 8. Positronium (Ps) formation cross-section with total cross-section.

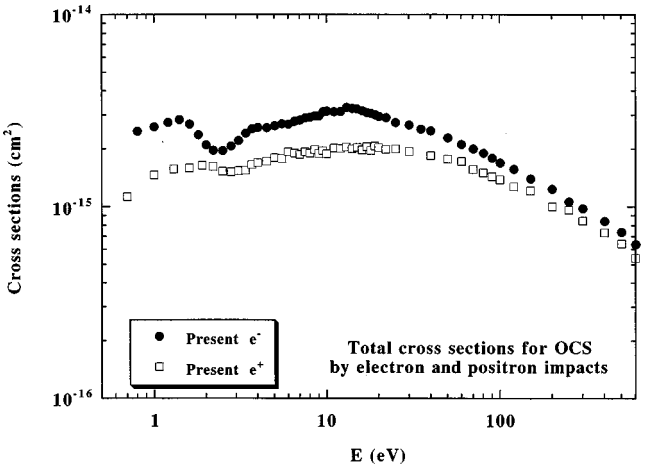

FIG. 9. A comparison in the total cross-sections by electron and positron scattering. We include only the present result, and that of Dababneh *et al.* (Ref. 12) for electron scattering as noted in the figure.

formation to the total cross-section is roughly 9.3%, while that for CO_2 is found to be 13.5%. This difference appears to be marginal, but may suggest that positron attachment is more likely for OCS, probably due to a larger number of electrons, rather than forming the Ps. The Ps formation is similar, in dynamics, to a charge-transfer process in ion–atom collisions, which is completely nonexistent for electron scattering. When an incoming positron is captured, at least temporarily, by a target electron charge distribution, rather than forming the Ps, then this process is regarded as a Ps formation within a molecule. And when there are more electrons in the target, it may be more likely that this process takes place.

C. Comparison between electron scattering and positron scattering

Figure 9 illustrates the comparison of both cross-sections by electron and positron impact by the present study. A few characteristic features, which are very interesting, should be noted speculatively: (i) the total cross-section by electron impact is consistently larger than that by positron impact at any collision energy. This is in marked contrast to the CO_2 case where the reversal of the cross-section takes place in the energy region between 0.7 and 2 eV. This reversal phenomenon in the cross-section has been observed for other systems[6] such as the NH_3 system, and may be due to the fact that rovibrational excitation becomes larger for positron scattering compared to that of electron scattering at a certain energy regime. It is to be noted that this larger cross-section for positrons might have a potential significance for applications. If positron impact can excite a certain type of a rovibrational motion or electronic state, and if these excited states connect with dissociation channels, this may lead to specific fragmentation products, which should be quite different from those by electron impact. Then, positron impact could be used for selective production of specific fragments or radicals of molecules since it is relatively easy to handle positron source and apparatus in a small laboratory. (ii) The total cross-section has a broad peak below 2 eV, and we speculate that the origin of the peak is likely positron attachment. In fact, for other larger molecules, a similar peak has been often observed, and as the molecular size increases, the more often and conspicuously the peak shows up.[6] (iii) At zero-energy limit, of course, these two cross-sections approach different values, based on scattering length theory; the knowledge of the exact energy region where these two cross-sections begin to diverge would provide a more accurate testing ground for interaction potentials. It is interesting that the 1.4 eV strong resonance in electron scattering coincides with a similar peak at nearly the same energy for positron scattering. This suggests that although the different energy dependence for the interaction between electron and positron with targets is expected, it appears that the two interaction schemes match accidentally. It is very interesting and practically important to search for resonances in positron scattering as a function of collision energy and in various types of scattering processes.

As discussed above, the reversals of the magnitude of the cross-section between electron and positron impact does not occur in any energy for OCS, while in CO_2, the total cross-section for positron impact becomes larger around 2 eV, but that for electron impact takes over below at around 0.8 eV. A possible contribution toward this reversal effect may be due to the rovibrational excitation for specific modes which is more efficient for positrons. Therefore, a comparative study of vibrational excitation between OCS and CO_2 is very interesting and important for understanding the phenomenon. Studies to elucidate the problem are underway.

IV. CONCLUSIONS

In summary, we have presented accurate total cross-sections for electron and positron scattering from OCS molecule. The present total cross-sections for electron impact agree extremely well with those by Dababneh *et al.* We have found that the total cross-section determined earlier by Szmytkowski *et al.* overestimates by a factor of two the peak in the 1.4 eV region although their data agree in energy dependence with the present results. The discrepancy is particularly pronounced at the resonance peak at 1.4 eV where

rovibrational excitation dominates. Therefore, we suggest thorough studies of vibrational excitation and electronic excitation processes in a wide range of collision energy, and based on these new accurate results, we will be able to establish a more comprehensive, complete, and correct set of cross-section data. For positron scattering, our knowledge of scattering mechanisms is quite limited and, particularly, that for any inelastic process is essentially nonexistent. Hence, more experimental studies for positron scattering should be carried out with a close theoretical analysis. Such studies have a potential for further discovery of interesting new phenomena. The CMS cross-sections are helpful; higher level calculations for molecules of this size are routinely done these days. Efforts to improve the level of these calculations are encouraged.

ACKNOWLEDGMENTS

The authors are much indebted to Dr. W. E. Kauppila for his communication of unpublished experimental results. The work has been supported in part by a grant from the Ministry of Education through Yamaguchi University, and by a grant-in-aid from the Ministry of Education, Science and Culture.

[1] M. Kimura, O. Sueoka, A. Hamada, M. Takekawa, Y. Itrikawa, H. Tanaka, and L. Boesten, J. Chem. Phys. **107**, 6616 (1997).
[2] M. S. Dababneh, Y.-F. Hsieh, W. E. Kauppila, C. K. Kwan, and T. S. Stein, XIV ICPEAC-Abstracts of Contributed Papers, Palo Alto, California, July 24–30, 1985, p. 230.
[3] A. Zecca, J. C. Nogueira, G. P. Karwasz, and R. S. Brusa, J. Phys. B **28**, 477 (1995).
[4] Cz. Szmytkowski, K. Maciag, G. Krzsztofowicz, and D. Filipovic, J. Phys. B **22**, 525 (1989).
[5] M. G. Lynch, D. Dill, J. Siegel, and J. L. Dehmer, J. Chem. Phys. **71**, 4249 (1979).
[6] M. Kimura, O. Sueoka, A. Hamada, and Y. Itikawa, Adv. Chem. Phys. (to be published).
[7] O. Sueoka, S. Mori, and A. Hamada, J. Phys. B **27**, 1453 (1994).
[8] K. R. Hoffman, M. S. Dababneh, Y.-F. Hsieh, W. E. Kauppila, V. Pol, J. H. Smart, and T. S. Stein, Phys. Rev. A **25**, 1393 (1982).
[9] A. Hamada and O. Sueoka, J. Phys. B **27**, 5055 (1994).
[10] The differential cross sections will be reported in a separate forthcoming paper.
[11] W. Sohn, K.-H. Kochem, K. M. Scheuerlein, K. Jung, and H. Ehrhardt, J. Phys. B **20**, 3217 (1987).
[12] H. Tanaka, L. Boesten, D. Matsunaga, and T. Kudo, J. Phys. B **21**, 1255 (1988).
[13] S. Srivastava, A. Chutjian, and S. Trajmar, J. Chem. Phys. **63**, 2659 (1975).
[14] R. T. Brinkman and S. Trajmar, J. Phys. E **14**, 24 (1979).
[15] M. Kimura and H. Sato, Comment At. Mol. Phys. **26**, 333 (1991).
[16] For vibrational excitation thresholds, we took the values from T. Shimanouchi, Tables of molecular vibrational frequencies, NSRDS-NBS 39 (1972).